Collection de notes internes de la Direction des Etudes et Recherches

UNE LOI DE COMPORTEMENT CYCLIQUE ELASTOPLASTIQUE AVEC UNE VARIABLE SEMI-DISCRETE ET UNE CONTRAINTE DE ROCHET

A THREE DIMENSIONAL ELASTOPLASTIC CYCLIC CONSTITUTIVE LAW WITH A SEMI DISCRETE VARIABLE AND A RATCHETTING STRESS

EDF Direction des Etudes et Recherches
Electricité de France

EDF
Electricité de France

Direction des Etudes et Recherches

SERVICE RÉACTEURS NUCLÉAIRES ET ECHANGEURS
Département Mécanique et Technologie des Composants

SERVICE INFORMATIQUE ET MATHÉMATIQUES APPLIQUÉES
Département Mécanique et Modèles Numériques

1995

GEYER P.
PROIX J.M.
JAYET-GENDROT S.
SCHOENBERGER P.
TAHERI S.

UNE LOI DE COMPORTEMENT CYCLIQUE ELASTOPLASTIQUE AVEC UNE VARIABLE SEMI-DISCRETE ET UNE CONTRAINTE DE ROCHET

A THREE DIMENSIONAL ELASTOPLASTIC CYCLIC CONSTITUTIVE LAW WITH A SEMI DISCRETE VARIABLE AND A RATCHETTING STRESS

Pages : 16

96NB00063

Diffusion : J.-M. Lecœuvre
EDF-DER
Service IPN. Département SID
1, avenue du Général-de-Gaulle
92141 Clamart Cedex

ISSN 1161-0611

SYNTHÈSE :

Dans une première partie, on décrit la modélisation en reliant les variables utilisées au comportement du matériau au niveau de la microstructure. L'algorithme utilisé pour implanter le modèle dans le Code Aster est brièvement présenté.

A partir d'une identification des paramètres du modèle effectuée sur des essais sous chargement uniaxial de traction-compression en contrainte et déformation imposées, on étudie les capacités du modèle.

1) on compare les résultats de simulation du modèle, dans le cas d'essais à déformations contrôlées non proportionnelles (circulaire, carré, un pas et deux pas d'escalier), avec les résultats expérimentaux et les simulations du modèle Benallal, pour lequel il y a un paramètre de non-proportionnalité qui a été obtenu par une identification non-proportionnelle.

2) On compare les résultats de simulation de la déformation progressive du modèle avec les essais du CEA sous traction constante, torsion alternée et les résultats obtenus avec le modèle de Burlet Cailletaud introduit dans le Code ASTER. Le modèle de Burlet Cailletaud possède 2 paramètres dédiés à la description de la déformation progressive sous chargement multiaxes identifiés sur les essais précédents. Les résultats de Burlet Cailletaud semblent globalement meilleurs, mais compte tenu du fait que notre modèle est identifié seulement sur le cas uniaxial, nous considérons que c'est un résultat honorable.

3) On compare les résultats de simulation de la déformation progressive avec un essai de rochet réalisé au département EMA de la DER en modifiant les paramètres du modèle.

L'ensemble de ces comparaisons montrent que le modèle proposé donne des résultats acceptables, malgré une identification seulement uniaxiale, tant qu'il y a suffisamment de plasticité à chaque cycle. Dans le cas où la plasticité est faible, en ce qui concerne la déformation progressive, le modèle surestime celle-ci, mais cette surestimation est moins importante que celle du modèle de Chaboche.

EXECUTIVE SUMMARY :

The study of cyclic elastoplastic constitutive laws is, at the moment, focused on non proportional loadings, but for uniaxial loadings some problems remain, as for example the ability for a law to describe simultaneously ratcheting (constant increment of strain) in non symmetrical ones.

We propose a law with a discrete memory variable, the plastic strain at the last unloading, and a ratchetting stress which, in addition to previous phenomena, describes the cyclic hardening in a push-pull test, and the cyclic softening after overloading. In the other hand the choice of all macroscopic variables is justified by a microscopic analysis. The extension to 3D situations of this law is proposed. The discrete nature of the memory leads to discontinuity problems for some loading paths, a modification is then proposed which uses a differential evolution law. For large enough uniaxial cycles, the uniaxial law is nevertheless recovered. An incremental form of the implicit evolution problem is given, and we describe the implementation of this model in the Code Aster a thermomechanical structural software using the f.e.m. developed at Electricité de France. For a 316 stainless steel we present comparisons between experiments and numerical results in uniaxial and biaxial ratchetting and non proportional strain controlled test (circular, square, stair loading).

A THREE DIMENSIONAL ELASTOPLASTIC CYCLIC CONSTITUTIVE LAW WITH A SEMI-DISCRETE VARIABLE AND A RATCHETTING STRESS

Geyer Ph.*, Jayet Gendrot S.*, Proix J. M.**,Shoenberger Ph.***, Taheri S.***
Electricité de France

*Direction des Etudes et Recherches, Les Renardières 77250 Moret sur Loing
**SEPTEN,12-14 Av. Dutrievoz 69628 Villeurbanne
***Direction des Etudes et Recherches,1 Av. Général de Gaulle, 92141, Clamart

1. INTRODUCTION

The study of cyclic elastoplastic constitutive laws is, at the moment, focused on non proportional loadings, but for uniaxial loadings some problems remain, as for example the ability for a law to describe simultaneously ratchetting (constant increment of strain) in non symmetrical load-controlled test, elastic and plastic shakedown in symmetrical and non symmetrical ones. We have proposed in [1] a law with a discrete memory variable, the plastic strain at the last unloading, and a ratchetting stress which, in addition to previous phenomena, describes the cyclic hardening in a push-pull test, and the cyclic softening after overloading. On the other hand the choice of all macroscopic variables is justified by a microscopic analysis. A modified law has been proposed in [2] to take into account the dependence of cyclic stress strain curve on the history of loading. The extension to 3D situations of this law is proposed in [3]. The discrete nature of the memory leads to discontinuity problems for some loading paths, a modification is then proposed which uses a differential evolution law. For large enough uniaxial cycles, the uniaxial law is nevertheless recovered. In [4] an incremental form of the implicit evolution problem is given, and we describe the implementation of this model in the *Code Aster*© [5] a thermomechanical structural software using the f.e.m, developed at Electricité de France. In this paper we briefly explain the model,and for a 316 stainless steel we present comparisons between experiments and numerical results in uniaxial ratchetting, non proportional strain controlled test (circular, square, stair loading), and constant traction with cyclic torsion tests.

2. THE MICROSTRUCTURE UNDER CYCLIC LOADING

When the cross slipping of dislocations is possible for a metal (easy cross slip for pure Al and pure Cu, difficult cross slip for a 316 stainless steel) the microscopic structure is characterized at low cyclic amplitude by permanent slip bands and at higher amplitude by cell structure, whose mean size decreases with an increasing amplitude of loading. But when the amplitude of loading decreases the cell structure is stable (at room temperature). The cell structure seems also to be detected for a monotonic loading. As before the cell size decreases with increasing strain. We suppose that the mean cell size is defined by the maximal stress supported by the material in its history. The asymptotic form of the curves showing mean cell size as a function of the amplitude of loading suggests us to suppose the existence of a minimal cell size depending only on the material and not on the loading. During cycling, dislocations pile up on the obstacles (walls), stabilization is obtained when the numbers of dislocations created and annihilated are equal. At stabilized state the plastic strain is created by dislocations which

sweep away the cell volume or P.S.B, and then are annihilated by dislocations of opposite sign. Once a stabilized state is obtained if we increase the amplitude of loading, smaller cells will be obtained. That means new obstacles are created on which dislocations have to be piled up again to obtain a new stabilized state. That means usually more than one cycle is needed to get a new stabilized state. This is macroscopically illustrated by a push-pull test. We call this: interaction between dislocation density and cell size. Different experiments show that at room temperature ratchetting is obtained (practically) at a nearly fixed maximal stress, independently of the amplitude of loading [6].This suggests the use of a cyclic ultimate stress S (ratchetting stress) which we relate to a minimal cell size. The idea of a threshold for ratchetting has been also used by other authors [7].

3 DEFINITION OF MACROSCOPIC VARIABLES THROUGH MICROSTRUCTURE

We define now more precisely the macroscopic variables in relation with the microscopic analysis:

- ε^p usual plastic part of the strain, related to the gliding of dislocations,
- σ_p maximal past absolute value of stress supported by the material in his history, related to the actual mean size of cells, this variable is used partly as $S - \sigma_p$ where S is the ratchetting stress.
- ε^p_n plastic deformation at the last unloading point. Here the significant variable is the difference $\varepsilon^p - \varepsilon^p_n$, on stabilized cycles. It measures the amplitude of plastic deformation, which may be related to sweeping of cell volume by the active dislocations
- λ cumulated plastic strain, related to the density of dislocations. But to take into account the interaction between cell size and dislocation density we use instead the variable $\lambda\,(1-\sigma_p/S)$

4 UNIAXIAL CONSTITUTIVE LAW.

4.1 Natural introduction of ε^p_n

In the case of ratchetting, after some cycles the tension and compression curves are translated at each cycle of a constant quantity. So we have (figure1):

$$\sigma_t=f\,(\varepsilon^p-\varepsilon^p_{2n}) \text{ and } \sigma_c=g\,(\varepsilon^p-\varepsilon^p_{2n+1}) \quad \text{with} \quad f',\ g'',g' >0 \text{ and } f''<0$$

where ε^p_{2n} (resp ε^p_{2n+1}) is the plastic strain at the last unloading on the compression (resp. traction) curve. These variables have been used in a different way in [8]. We suppose that there is no ratchetting phenomena for a symmetric loading, (for $\sigma_{min}=-\sigma_{max}$, we obtain plastic or elastic shakedown). It is so possible to show that the general form of tension and compression curves in the ratchetting state are:

$$\sigma_t=(\varepsilon^p-\varepsilon^p_{2n})\,*Q(|\varepsilon^p-\varepsilon^p_{2n}|)+R(|\varepsilon^p-\varepsilon^p_{2n}|)$$
$$\sigma_c=(\varepsilon^p-\varepsilon^p_{2n})\,*Q(|\varepsilon^p-\varepsilon^p_{2n+1}|)-R(|\varepsilon^p-\varepsilon^p_{2n+1}|)$$

We studied the case Q=0 in [1]. It has been shown in this case that the law may des-

cribe the following phenomena: the ratchetting in non symmetrical load-controlled test, elastic and plastic shakedown in symmetrical and non symmetrical one, the cyclic hardening in a push-pull test, the cyclic softening after overloading and also the dependence of cyclic-stress-strain-curve on the history of loading. However the difficulty in this case comes from the bad representation of the cyclic-stress-strain-curve after prehardening, and also the linear relation between mean stress and mean strain.

The case Q=K (K a non zero constant) is described in [2] and is the model which is used for the simulation. However a better result may probably be obtained by a non linear function. We have so:

$$\sigma_t = K\,(\varepsilon^p - \varepsilon^p_{2n}) + R(|\varepsilon^p - \varepsilon^p_{2n}|)$$
$$\sigma_c = K\,(\varepsilon^p - \varepsilon^p_{2n+1}) - R(|\varepsilon^p - \varepsilon^p_{2n+1}|)$$

This obviously remembers the yield function with combined kinematic isotropic hardening in 3D situation:

$$\sqrt{\frac{3}{2}\sum_{ij}\left(s_{ij}-x_{ij}\right)\left(s_{ij}-x_{ij}\right)} - R = 0$$

which gives in uniaxial case

$\sigma_t = 1.5\,x_{11} + R$ in tension and $\sigma_c = 1.5\,x_{11} - R$ in compression.

4.2 Introduction of a ratchetting stress S

We suppose that in the uniaxial case ratchetting (constant increment) is obtained when the maximal stress (or minimal stress in absolute value) reaches the value S [2]. But for the stresses smaller than this value we have elastic or plastic shakedown. The simplest way to obtain this is to transform the expression

$K(\varepsilon^p - \varepsilon^p_{2n})$ into $K(S^*\varepsilon^p - \sigma_p{}^*\varepsilon^p_{2n})$ where σ_p is the maximal stress obtained during the history of loading. The expression of tension and compression curves in the case of plastic shakedown are so:

$$\sigma_t = K\,(S*\varepsilon^p - \sigma_p*\varepsilon^p_{2n}) + R(|\varepsilon^p - \varepsilon^p_{2n}|)$$
$$\sigma_c = K\,(S*\varepsilon^p - \sigma_p*\varepsilon^p_{2n+1}) - R(|\varepsilon^p - \varepsilon^p_{2n+1}|)$$

It is possible to describe schematically the obtention of ratchetting and plastic shake down. In fact the above two relations constitute a recurrent one. For $X=\varepsilon^p_{2n}$, $Y=\varepsilon^p_{2n+1}$, we get two curves:

$$C1 <=> K.(SY - \sigma_p X) + R(|Y-X|) - \sigma_{max} = 0,$$
$$C2 <=> K.(SY - \sigma_p X) - R(|Y-X|) - \sigma_{min} = 0$$

For $S > \sigma_p$, C1 and C2 are two intersecting curves and with an initial state of strain ε^p_0, plastic or elastic shakedown is obtained (figure 2). For $S=\sigma_p$, C1 and C2 are two parallel lines and ratchetting is obtained. However if $\sigma_{max}=-\sigma_{min}$ the two lines are superposed and plastic or elastic shakedown is obtained.

4.3 Introduction of cumulated plastic strain λ

The introduction of this variable permits to get the hardening and the softening for strain controlled tests. However in a strain controlled test once stabilization is obtained for a greater amplitude of strain the stabilization will be obtained in one cycle. This difficulty will be surrounded if we use instead of λ the parameter $\lambda(1-\sigma_p/S)$. Finally as the simplest choice [2] we may take:

$$\sigma_t = K(\lambda(1-\sigma_p/S))\,(S*\varepsilon^p - \sigma_p*\varepsilon^p_{2n}) + f(\lambda(1-\sigma_p/S))\,R(|\varepsilon^p - \varepsilon^p_{2n}|),$$

$$\sigma_c = K(\lambda(1-\sigma_p/S))\,(S*\varepsilon^p - \sigma_p*\varepsilon^p_{2n+1}) - f(\lambda(1-\sigma_p/S))\,R(|\varepsilon^p - \varepsilon^p_{2n+1}|)$$

4.4 Cyclic stress strain curve

The usual cyclic stress strain curve for a symmetrical loading is given by:

$$y = (1.5K_\infty S\,x + R(2x)) / (1-1.5K_\infty.x)$$

where $y=\Delta\sigma/2$, $x=\Delta\varepsilon^p/2$, and $x < (1/1.5\,K_\infty\,x)$, and $K_\infty=K(\lambda=\infty)$. If there is a prehardening σ_p, the cyclic curve is given by:

$$y = 1.5\,K_\infty\,(S+\sigma_p)x + R(2x)$$

4.4 Relation between σ_{mean} and ε^p_{mean}

We have $\sigma_{mean}=1.5K_\infty\,(S-\sigma_p)\,\varepsilon^p_{mean}$ this gives a possibility of a good relaxation for important prehardening, which seems being the case for 316 stainless steel.

5. THREE-DIMENSIONAL LAW

The extension to three dimensional situations of the previous uniaxial law encounters two main difficulties. First, choices have to be made on the variables themselves. For the sake of simplicity as frequently done, the deviatoric part of the tensors is chosen to keep the uniaxial law's general form. The constitutive law is now simply described by an elastoplastic model where yield function combines isotropic and kinematic hardening:

$$F(\sigma, \varepsilon^p, \lambda, \sigma_p, \varepsilon^p_n) = |\sigma_D - \mathbf{X}(\varepsilon^p, \varepsilon^p_n, \lambda, \sigma_p)| - R(\lambda, \sigma_p, |\varepsilon^p - \varepsilon^p_n|)$$

The usual normality and consistency relations are used for the remaining variables ε^p and λ [3]. But a difficulty arises from extension of the definitions and evolution equations of the memory variables σ_p and ε^p_n. As a matter of fact, the uniaxial loadings histories are very poor: there is no tangent loadings, cycling is only defined by two extreme values etc. Intrinsic definitions and more precise evolutions laws are then needed in the 3D case. The variable σ_p is defined as the maximal past deviatoric norm of the stress experienced by the material - the norm is denoted by $|\sigma_D|$ - With initial value

σ_p° of σ_p, the precise definition is:

$$\sigma_p(t) = \left(\max_{u \in [0,t]}\right)\left(\sigma_p^\circ, |\sigma_D(u)|\right)$$

and we can rewrite this definition as a new yield function G in the deviatoric stress space:

$G(\varepsilon^p, \lambda, \sigma_p, \varepsilon^p_n) = \sigma_p - |X1(\varepsilon^p, \lambda, \sigma_p)| - R1(\lambda, \sigma_p, |\varepsilon^p_n - \varepsilon^p|)$

leading to the evolution equation for σ_p (H is the Heviside function):

$$\dot{\sigma}_p = H\left(|\sigma_D| - \sigma_p\right)\frac{\sigma_D \dot{\sigma}}{|\sigma_D|}$$

Two problems arise from the definition of the evolution law of ε^p_n [3]. The first one is that the material behavior admits some undershooting of the monotonic stress-strain curve after an elastic unloading followed by reloading. However this is not always a disadvantage (see discussion). The second problem, more important from a physical point of view, is the requirement of continuity of the stress-strain curve with respect to very small unloadings. With full discrete memory, this requirement is generally not fulfilled: any unloading, even as small as possible, leads to an (discontinuous) evolution of the memory variable which induces in turn a discontinuity on the value of the yield function F. This last discontinuity can finally causes the violation of the yield condition $F \leq 0$.

For 3D loading paths, this problem is of primary importance because *micro-unloadings* can result from changes of direction of the loading path in the stress space.To overcome this last difficulty, we modify the discrete evolution law for ε^p_n to a semi discrete one - the word semi-discrete is used because of the saturation of the memory ensuing from the definition of the evolution -. Starting from the discrete model:

$$\Delta\varepsilon^p_n = \varepsilon^{p+}_n - \varepsilon^{p-}_n = \varepsilon^p - \varepsilon^{p-}_n \qquad \text{if} \qquad F = 0 \qquad \left(\dot{\sigma}\frac{\partial F}{\partial \sigma}\right) \leq 0$$

we introduce a scalar differential evolution equation together with a consistency condition ensuring the fulfillment of the yield condition:

$$\dot{\varepsilon}^p_n = \alpha\left(\varepsilon^p - \varepsilon^p_n\right) \qquad \text{if} \qquad F = 0 \qquad \left(\dot{\sigma}\frac{\partial F}{\partial \sigma}\right) \leq 0$$

$$\alpha \geq 0 \qquad \alpha F = 0 \qquad F \leq 0$$

It can be seen that, with appropriate *generalized hardening conditions* on the yield function F we have [3]:

- the yield condition ($F < 0$) is never violated,
- the continuity with respect to the chronology parameter is restored,
- the memory shows a *saturation effect*: when, during the unloading, the value of ε^p_n reaches ε^p, then ε^p_n stays at this value and the unloading becomes purely elastic with no internal variable evolution,
- for uniaxial cycling loadings, the discrete memory is recovered between two successive unloadings, provided the cycle is large enough.

6. THE IMPLICIT INTEGRATION OF THE 3D RATES EQUATIONS

When $|\sigma_D|$ does not reach σ_p the law reduces - in loading evolutions - to the standard plasticity laws. Non standard flow rules are obtained when σ_p varies during loading (but normality for the rate of ε^p still remains). To write down extensively the proposed constitutive law, we present hereafter its implicit incremental form which will be used in computations.

We denote by **e** the "state" $(\varepsilon^p, \lambda, \sigma_p, \varepsilon^p_n)$, by **A** the elasticity tensor and by **X** the backstress tensor. In order to integrate rate equations of the constitutive model over the increment Δt: we integrate the flow rule by the backward difference scheme:

$$\Delta\varepsilon^p = \Delta\lambda \frac{\partial F}{\partial \sigma_{t+\Delta t}}$$

- we impose respect of the yield function F when plasticity occurs, at the end of increment: $F_{t+\Delta t} = 0$
- equations of elasticity are written at the end of increment: $\sigma_{t+\Delta t} = \mathbf{A}_{t+\Delta t}\ \varepsilon^e{}_{t+\Delta t}$
- rate of ε^p_n is integrated by the forward difference scheme in order to respect $\varepsilon^p{}_{nt+\Delta t} = \varepsilon^p{}_{nt} + \Delta\varepsilon^p{}_n = \varepsilon^p{}_t$ at the end of increment, so we have:

$$\Delta\varepsilon^p{}_n = \Delta\alpha\ (\varepsilon^p - \varepsilon^p{}_n)_t$$

- we impose respect of the *pick function* G when σ_p varies during loading:

$$G_{t+\Delta t} = \sigma_{pt+\Delta t} - |\mathbf{X}|_{t+\Delta t} - R_{t+\Delta t} = 0$$

So, we can exhibit four types of increment for this model, by opposition with the two states, elastic and elasto-plastic, of a standard plasticity model:

- A *Purely Elastic* increment (E), where only the variable σ is incremented,
- A *Pseudo-Elastic* increment (PE), where ε^p_n and σ are actualized,

$$\begin{aligned} &\Delta\varepsilon^p_n = \Delta\alpha\left(\varepsilon^p - \varepsilon^p_n\right)_t \\ &\sigma_{t+\Delta t} = \mathbf{A}_{t+\Delta t}\left(\varepsilon_{t+\Delta t} - \varepsilon^p_t\right) \qquad (S1) \\ &F\left(\sigma_{t+\Delta t}, \varepsilon^p_{nt+\Delta t}, \varepsilon^p_t, \sigma_{pt}, \lambda_t\right) = 0 \end{aligned}$$

- An *Elasto-Plastic* increment (EP), where σ, λ and ε^p are actualized,

$$\begin{aligned} &\sigma_{t+\Delta t} = \mathbf{A}_{t+\Delta t}\left(\varepsilon_{t+\Delta t} - \varepsilon^p_t - \Delta\lambda\frac{\partial F}{\partial \sigma_{t+\Delta t}}\right) \qquad (S2) \\ &F\left(\sigma_{t+\Delta t}, \varepsilon^p_{nt}, \varepsilon^p_{t+\Delta t}, \sigma_{pt}, \lambda_{t+\Delta t}\right) = 0 \end{aligned}$$

- And a *Pseudo-Elasto-Plastic* increment (PEP), where σ, λ, ε^p and σ_p are actualized.

$$\sigma_{t+\Delta t} = A_{t+\Delta t}\left(\varepsilon_{t+\Delta t} - \varepsilon^p_t - \Delta\lambda\frac{\partial F}{\partial \sigma_{t+\Delta t}}\right)$$

$$F\left(\sigma_{t+\Delta t}, \varepsilon^p_{nt}, \varepsilon^p_{t+\Delta t}, \sigma_{pt}, \lambda_{t+\Delta t}\right) = 0 \qquad (S3)$$

$$G\left(\varepsilon^p_{nt}, \varepsilon^p_{t+\Delta t}, \sigma_{pt+\Delta t}, \lambda_{t+\Delta t}\right) = 0$$

The integration algorithm first makes an *elastic prediction*, in order to decide if the increment is (E)/(PE) or (EP)/(PEP), and then makes a *plastic prediction* to choose between (EP) or (PEP) integration.The algorithm presented hereafter has been implemented in the ***Code Aster*** ©, developed at *Electricité de France* [5]. The three non linear implicit systems of tensorials equations (S1,S2,S3) are solved by a Newton method.

7 COMPARISON WITH EXPERIMENTS

We use the following definition for isotropic and kinematic hardenings:

$$R = D\left(A\left|\varepsilon_p - \varepsilon^n_p\right|^\alpha + R_o\right) \qquad C = C_\infty + C_1 e^{-b\lambda\left(1-\frac{\sigma_p}{S}\right)} \qquad D = 1 - me^{-b\lambda\left(1-\frac{\sigma_p}{S}\right)}$$

$$X = C\left(S\varepsilon_p - \sigma_p\varepsilon^n_p\right)$$

Two types of comparison with experimental data are presented for a 316 stainless steel.

A) Identification is done only on uniaxial curves from some references, but the comparison with non proportional data is done on other references. This is to test the robustness of the method.
B) Identification is done on uniaxial or non proportional loadings for some loading amplitudes. The comparison is done for other values of loading amplitude from the same reference. This is to test the precision of the method. In this case only a uniaxial identification is presented.

7.1 Case A

For the identification uniaxial strain controlled tests and stress controlled tests have been used (figure 3,a, 3b) [9]. The parameters are:

$S = 800$ MPa	$A = 341$ MPa	$C_\infty = 5,8$	$R_0 = 150$ MPa
$C1 = 6,8$	$m = 0,264$	$\alpha = 0,122$	$b = 11$

Figure 4,5,6,7 (**a** and **b**) show the results of simulation obtained by our model for circular, square, one-step, and two-step loading ($\Delta\varepsilon$ =0.8%). On figures 4,5,6,7 (**c** and **d**)are presented at stabilized state the experimental data (dashed lines), and also simulation obtained by a model presented in [10], where non proportional experiments have been used for identifications. The amplitude of loading in circular case is $\Delta\varepsilon$ =1%. Figures 8a,8b,8c,8d present the results for constant tension and symmetrical cyclic torsion (strain controlled) tests. We compare the experimental data [11], with simulations

obtained by our model, and two other constitutive laws. The first one is a Chaboche model with two kinematical variables [12]. The second one is a two kinematical Chaboche law modified by introduction of a radial evanescent memory [13], [14]. It worths noting that for this second model the tests 30,35,36 have been used for identifications.

7.2 Case B

Experimental program

An experimental program has been conducted to investigate the behavior of an 316 austenitic stainless steel under cyclic load generating ratchetting at 20 and 350 °C [15]. Here are only presented the results at 20 °C.

Material : The material used is a 316L stainless steel, with controlled nitrogen. The final heat treatment consisted in a holding at 1100 C during one and half hour, followed by water quench. All specimens were taken from a 30mm thick plate, in the rolling direction and at mid-thickness. The chemical composition and tensile properties are given in the following tables.

Table 1: chemical composition, wt%

C	S	P	Si	Mn	Ni	Cr	Mo	N	B	Co	Cu
0.03	0.001	0.021	0.44	1.84	12.3	17.54	2.47	0.075	0.0011	0.15	0.175.

Table 2: tensile properties of material

Temperature	0.2% yield stress	Ultimate stress	Elongation	Reduction in area
20 °C	264 MPa	591 MPa	61%	86%

*Experimental procedure:*The ratchetting tests were carried on smooth cylindrical specimens with length and diameter of 16 and 8 mm respectively. The specimens were subjected to a force controlled cyclic solicitation applied by a servo-mechanical machine. A triangular wave and a frequency of 0.2 Hz were used. We did incremental multilevel tests with constant amplitude and increasing mean stress.

Results: These results have shown with the same criterium as in [6] (it is supposed that ratchetting is obtained, if between the 50th and 100th cycles the increment over the 50 cycles is greater than 0.1%) that at room temperature the obtention of ratchetting is only dependent on maximum stress, while that is not the case at 350 °C. Neverthless after 2000 cycles a tendancy to plastic shakedown is remarked [15]. This is on agreement with the fact that in our model parameter S is high enough so that ratchetting is never obtained for in service loadings. These experimental results show also that for a symmetrical stress controlled test there may be positive ratchetting or negative ratchetting, begining with the same direction of loading (four experiments have been realized at 350 MPa). So the hypothesis (as for this model) that a symmetrical loading in stress controlled test gives a symmetrical response in strain seems acceptable.

Comparison with simulation:

Are repported on figure 9 two types of simulation. For the first one (basic identification)- the parameters of case A have been used. For the second one a new identification is done on a part of the parameters. We take:

$$S = 1080\,\text{MPa} \qquad A = 400\,\text{MPa} \qquad \alpha = 0,127 \qquad C_{\infty} = 0,5$$

8 DISCUSSION

The figure 10 shows the case where there is no plasticity in compression. That may be also the case after an elastic shakedown. The calculation must be stopped automatically in this case. However this is not actually programmed and the strain increase continue until stabilization.This gives an overestimating of maximal strain for small amplitude of loading when there is a possibility of elastic shakedown. It is possible to modify the software to stop automatically the calculus in the case of an elastic shake down. However this is not done, essentially because this model originally has been proposed to reproduce the behavior of the 316 stainless steel. This steel present a cold creep at room temperature. We hope that this overestimating is sufficient enough to prevent the addition of a creep deformation to elastoplastic deformation (in the case where secondary creep is negligable).

REFERENCES

[1] Taheri S.,1989. Une loi de comportement uniaxial cyclique avec variable àmemoire discrete. 9ème Congrés Francais de mécanique, Metz, France.

[2] Taheri S.,1991. A uniaxial cyclic elasto-plastic constitutive law with a discrete memory variable. SMIRT 10, L22, Tokyo, Japan.

[3] Andrieux S. Taheri S., 1992. A cyclic constitutive law for metal with a semi-discrete memory variable for description of ratchetting phenomen. Rapport E.D.F/D.E.R/HI-71/7814.

[4] ***Code Aster*** ©v.2,(1992). Analyse des structures et thermo-mécanique pour des études et des recherches. Manuel d'utilisation / Manuel de descriptif Informatique / Manuel de référence.E.D.F/D.E.R.

[5] Andrieux S., Shoenberger Ph.,Taheri S., 1993, A three dimensional cyclic constitutive law for metal with a semi-discrete memory variable SMIRT 11, L22, Stuttgart, Germany.

[6] Pellissier-Tanon A.,Bernard J.L, Amzallag C., Rabbe P.1980. Evaluation of the resistance of type 316 stainless steel against progressive deformation.Int Sym. on low-cycle fatigue and life prediction, Firminy, France.

[7] Chaboche J. L. 1991. On some modifications of, kinematical hardening to improve the description of ratchetting effect. Int. J. of Plasticity Vol. 7 P. 661-678.

[8] Guionnet Ch. 1989. Modelisation de la deformation progressive dans les essais biaxiaux. Rapport CEA - DEMT/89 - 120.

[9] Geyer Ph., Proix J.M., Shoenberger Ph., Taheri S., 1993 . Modeling of ratchetting. Collection de notes internes DER. 93NB00153.

[10] Benallal A. 1989. Thermoviscoplasticité et endommagement des structures. These de Doctorat es sciences, universite Paris 6.

[11] Cousseran P., Lebey J., Roche R., Corbel P. ,1980. Essais de déformation progressive de l'acier inoxydable 316L à la temperature ambiante. Rapport CEA-N-2139.

[12] Engel J. J., Rousselier G. 1985 . Comportement en contrainte uniaxiale sous chargement cyclique de l'acier inoxydable austenitique 17-12 Mo à très bas carbone et azote controlé. EDF/DER, rapport HT/PCD 599 MAT T 43.

[13] Burlet H., Cailletaud G. 1987. Modelling of cyclic plasticity in finite element codes, 2th Int. Conf. on constitutive laws for engineering materials, theory and application, Tucson, Arizona.

[14] Geyer Ph. 1993 . Modélisation des phénomènes de déformation progressive par le modèle élastoplastique de Chaboché modifié par Burlet et Cailletaud. EDF/DER/rapport HT26/93/052A.

[15] Jayet-Gendrot. S. 1994, Repport to be published.

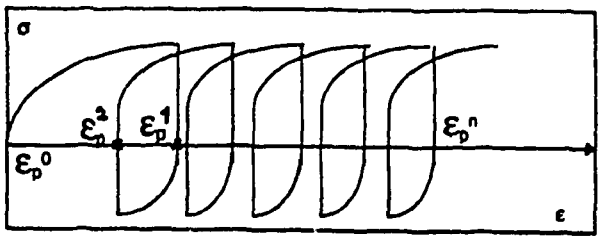

Figure 1 Definition of ε^p_n

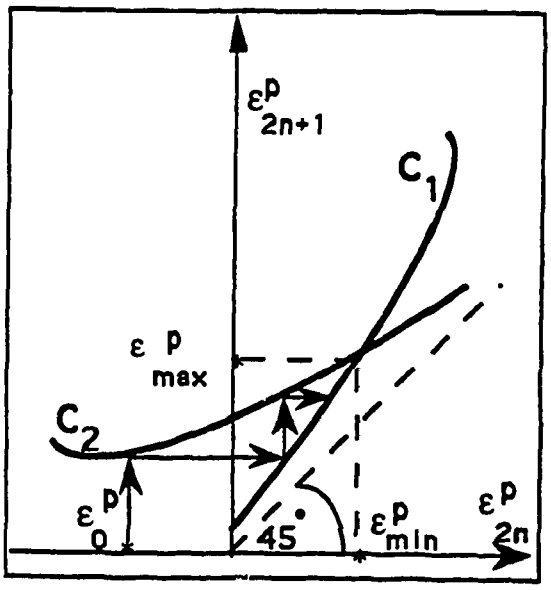

Figure 2 Plastic shakedown

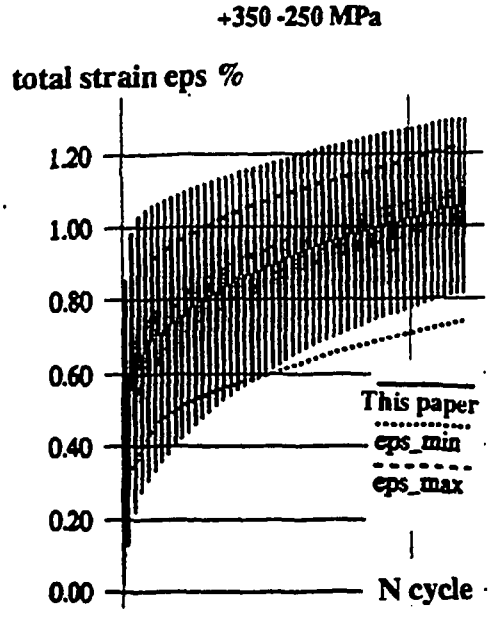

Figure 3a Uniaxial stress controlled test used for basic identification

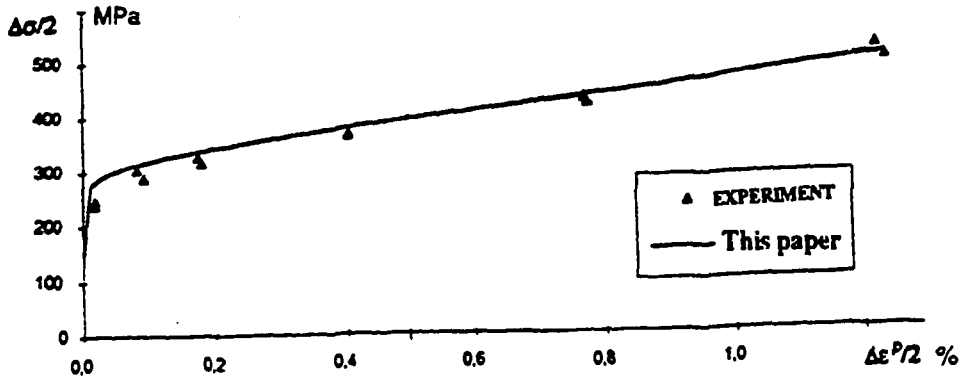

Figure 3b Cyclic stress strain curve used for basic identification

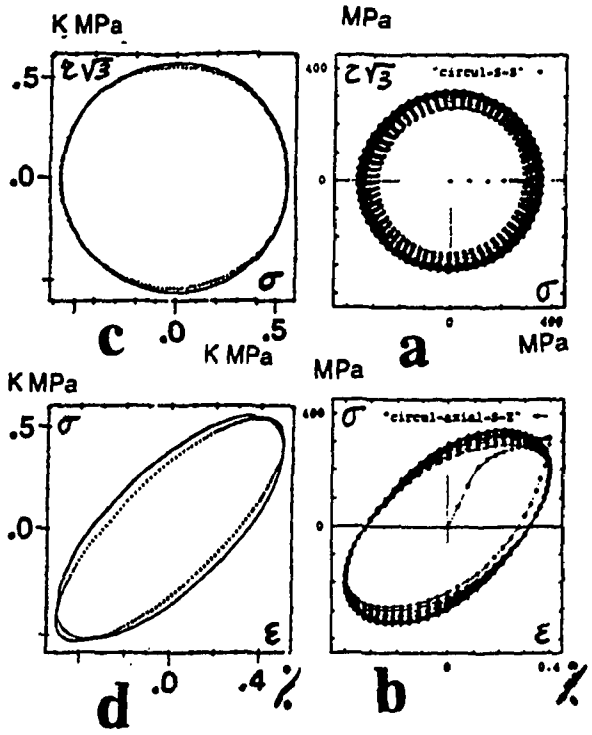

Figure 4 Circular loading

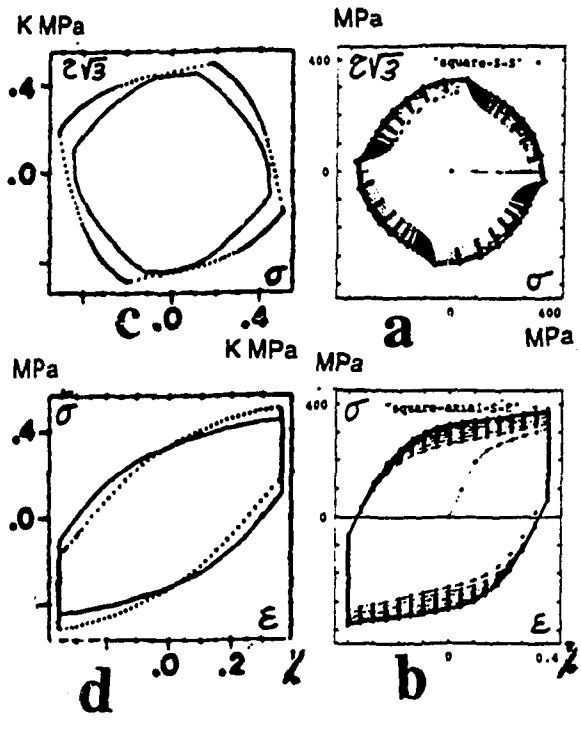

Figure 5 Square loading

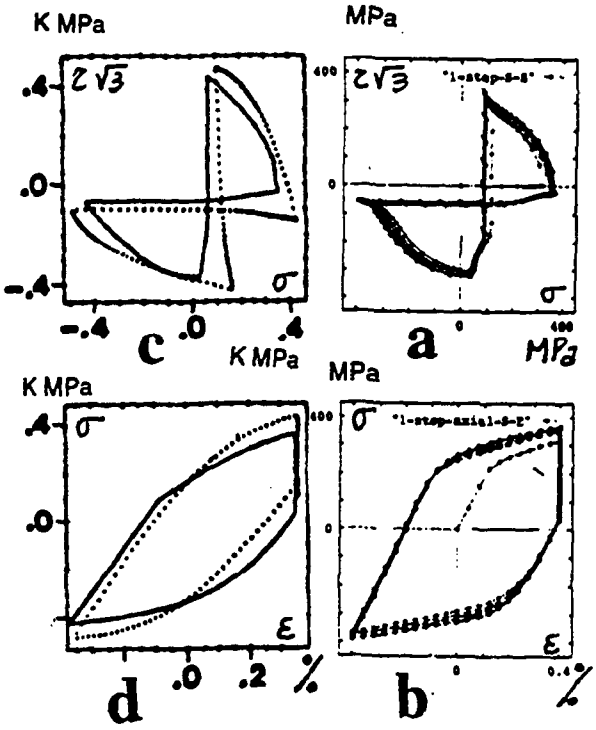

Figure 6 1-step loading

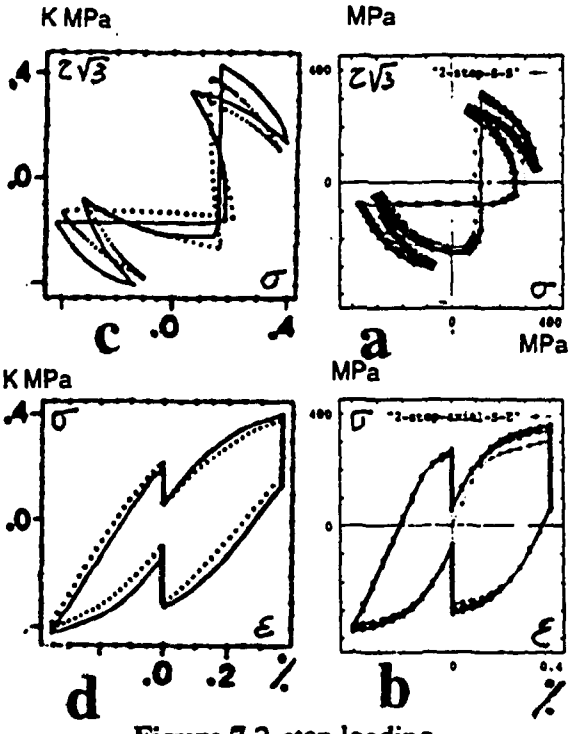

Figure 7 2-step loading

a,b : Simulations This paper. only uniaxial identification used
c,d : Stabilized state, Experiment [10] ----------
c,d : Stabilized state, Simulation [10] ——— non proportional identification used :

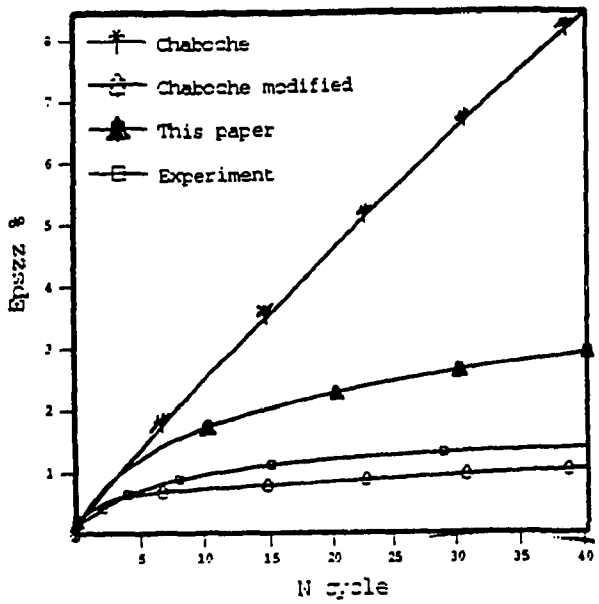

Test 30

Figure 8b σ_{zz}=157 MPa, $\varepsilon_{\theta z}$= 0.2%

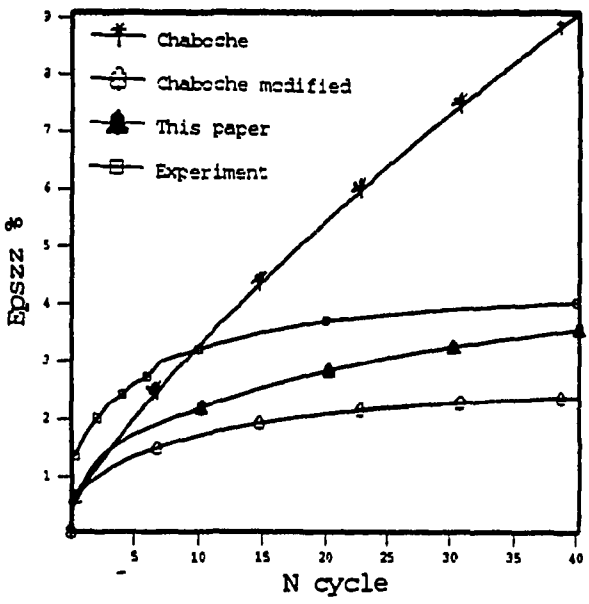

Test 29

Figure 8a σ_{zz}=286 MPa, $\varepsilon_{\theta z}$= 0.1%

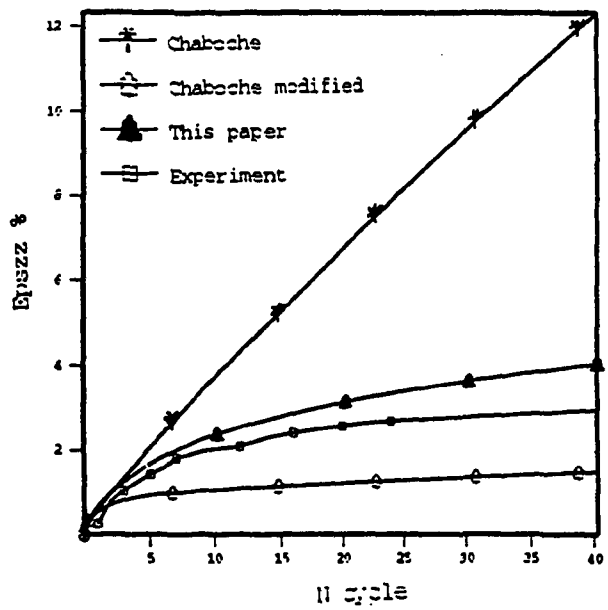

Test 36

Figure 8d σ_{zz}=204 MPa, $\varepsilon_{\theta z}$= 0.2%

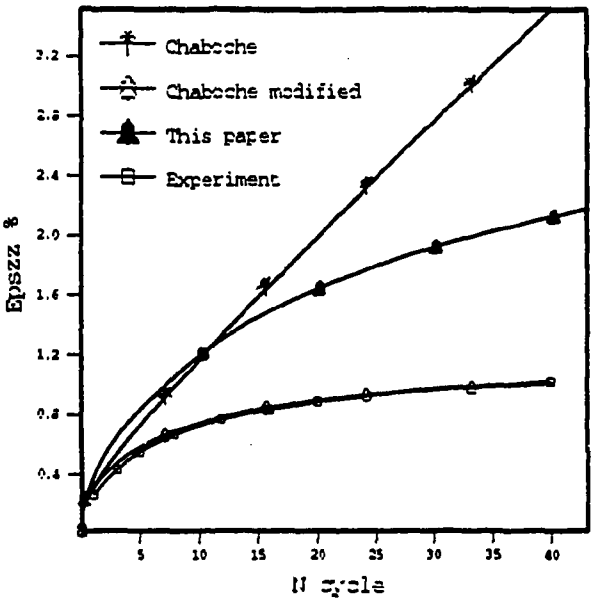

Test 35

Figure 8c σ_{zz}=204 MPa, $\varepsilon_{\theta z}$= 0.1%

Figure 8 CONSTANT TENSION CYCLIC TORSION TESTS

This paper	only uniaxial identification used
Chaboche	only uniaxial identification used
Chaboche modified	non proportional identification used :
Experiment [11]	

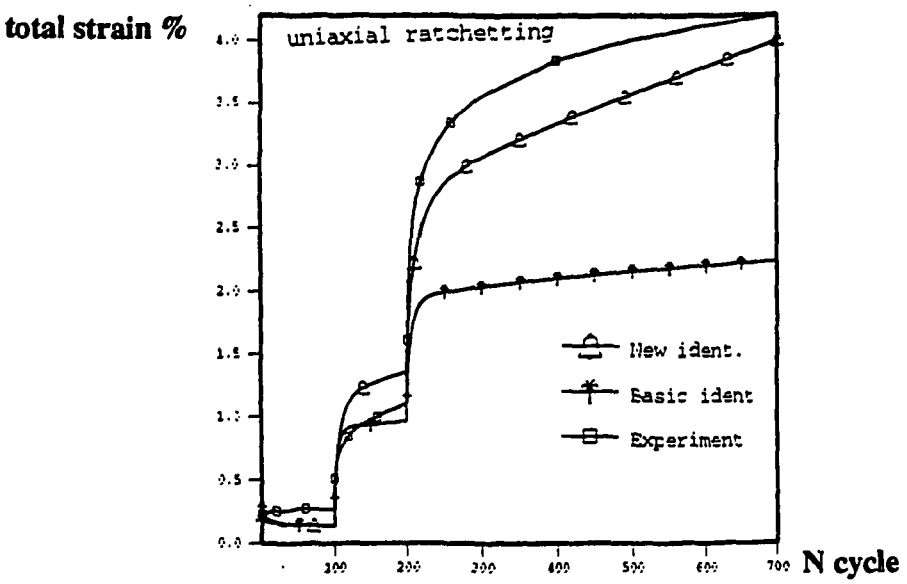

Figure 9 Comparison simulation, experiment

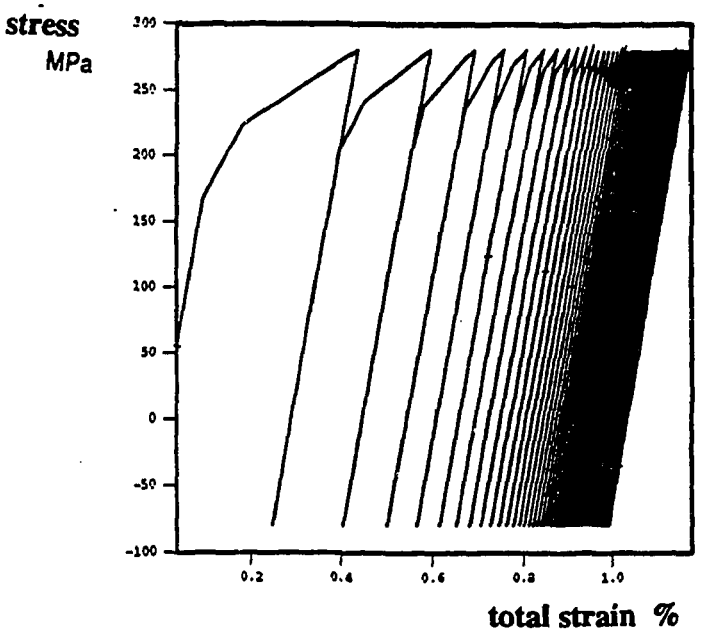

Figure 10 Overestimating of strain after elastic shakedown